Cancer Imaging (2006) **6,** 33–42
DOI: 10.1102/1470-7330.2006.0007

CI

e-med
www.e-med.org.uk

ARTICLE

New MR techniques for the detection of liver metastases

J Ward

Department of Clinical Radiology, St James's University Hospital, Leeds, UK

Corresponding address: Janice Ward, Department of Clinical Radiology, St James's University Hospital, Beckett Street, Leeds LS9 7TF, UK. E-mail: janice.ward@leedsth.nhs.uk

Date accepted for publication 6 February 2006

Abstract

It is well established that hepatic resection improves the long-term prognosis of many patients with liver metastases. However, incomplete resection does not prolong survival, so knowledge of the exact extent of intra-hepatic disease is crucially important in determining patient management and outcome. MR imaging is well recognised as one of the most sensitive methods for detecting metastases. Recent developments in gradient coil design, the use of body phased array coils and the availability of novel MR contrast agents have resulted in MR being recognised as the pre-operative standard in this group of patients. However, diagnostic efficacy is extremely dependent on the choice and optimisation of pulse sequences and the appropriate use of MR contrast agents. This article reviews current MR imaging techniques for the detection and characterisation of metastases and discusses the relative capability of different techniques for detecting small lesions.

Keywords: *Liver, MR; magnetic resonance, pulse sequences; magnetic resonance technology; magnetic resonance, three-dimensional; MR contrast agents; MR comparative studies; liver neoplasm, metastases; liver neoplasm, MR.*

Introduction

In patients with liver metastases from colorectal cancer hepatic resection has proven survival benefits and is curative in a small proportion of cases. Patients whose metastases are small, few in number and metachronous have the best prognosis, but there is now good evidence that patients with more extensive disease can benefit from resection[1–4]. The number, size and distribution of lesions are no longer limiting factors, provided all lesions are removed with adequate tumour-free margins and there is sufficient normal liver to maintain liver function postoperatively. Survival benefits are also well established in patients with neuroendocrine metastases and in a minority of patients with localised metastases from other primary sites which have a more indolent course[5,6]. Treatment success, however, depends on the removal of all sites of intra-hepatic disease and the absence of disease outside the liver; incomplete resection does not prolong survival. Consequently, more patients are being referred for preoperative assessment and, since many have multiple small lesions, the role of imaging is increasingly challenging. Almost all metastases larger than 1 cm are demonstrated with current imaging techniques but the detection of smaller lesions is still relatively poor[7–11]. Although the primary modalities for liver imaging are ultrasound and CT, recent studies have suggested that contrast-enhanced MRI is the most sensitive method for detecting small metastases and MRI is now considered the preoperative standard[12–16]. Moreover, recent developments in MRI hardware and software and the availability of novel MRI contrast agents have improved small lesion detection[13–25].

This article considers the current status of MR imaging techniques in the detection and characterisation of liver metastases and discusses the technical requirements for optimum performance. The accuracy and relative capability of various MR techniques for detecting sub-cm lesions is emphasised.

This paper is available online at http://www.cancerimaging.org. In the event of a change in the URL address, please use the DOI provided to locate the paper.

1470-7330/06/010033 + 10

© 2006 International Cancer Imaging Society

Unenhanced sequences

MR performance is primarily dependent on technique and the optimisation of pulse sequences. To date, liver MR has been most successful at a field strength of 1.5 T using high performance gradients, phased array multicoils and optimised imaging parameters [26,27]. Signal-to-noise ratio (SNR) is influenced by field strength and surface coil configuration whilst imaging speed and spatial resolution are influenced by gradient performance. With stronger gradient systems fast breathhold sequences with T1 and T2 weighting have become routine and motion-induced artifacts are no longer a significant problem. We recommend using breathhold sequences wherever possible since they are the most effective means of eliminating motion artifact. Moreover, breathhold versions of traditionally used sequences have been shown to have superior image quality and to be at least as good as non-breathhold versions for lesion detection [28,29].

Unenhanced sequences are an important part of any MR examination. They are essentially used to characterise lesions and identify fatty change. Lesion signal intensity (SI) on unenhanced T1w and T2w images often provides an indication of the type of lesion and guides the selection of contrast media for a more definitive diagnosis. T2w images determine the fluid content of lesions and are invaluable for distinguishing solid and non-solid tumours. We currently use a single shot fast spin echo (FSE) sequence with half-fourier reconstruction (HASTE) because motion artifacts are consistently absent even during free breathing and small cysts and fluid collections are well defined. In-phase (IP) and opposed-phase (OP) T1w GRE imaging (chemical shift imaging) provides a definitive diagnosis of focal or diffuse fatty infiltration [30]. This is particularly important when patients are being considered for hepatic resection since fatty change—frequently seen in patients following chemotherapy—may compromise hepatic function postoperatively. The fatty liver has a clearly reduced SI on OPT1w compared with IPT1w images, so whilst the detection and characterisation of liver lesions by ultrasound and CT is handicapped by fatty change, chemical shift MR imaging allows accurate differentiation of metastases and focal fatty change or focal sparing in a fatty liver.

In terms of lesion detection, low lesion-to-liver contrast on unenhanced sequences has resulted in rather poor detection rates for sub-cm metastases [27]. Low-contrast lesions are particularly inconspicuous on breathhold T2w FSE sequences and are often better depicted on T1w images (Fig. 1). Low liver-to-lesion contrast on FSE is multifactorial. FSE is insensitive to susceptibility so liver signal is slightly higher than with conventional spin echo imaging; magnetisation transfer (MT) effects which cause solid lesions to lose SI are particularly marked on multi-slice FSE sequences and become more pronounced with increasing echo train length; and FSE is also subject to blurring of short T2 tissues because most of the high spatial frequencies are collected at the later echoes when there is relatively little remaining signal. Of the unenhanced sequences, breathhold STIR is probably the most sensitive for depicting metastases [31] although image quality is variable. The additive effects of T1 and T2 provide strong image contrast which improves the conspicuousness of small lesions (Fig. 1), but phase artifacts may be severe at longer TEs.

Dynamic gadolinium-enhanced imaging (DGEI)

Rapid sequential imaging with extra-cellular space (ECS) gadolinium (Gd)-based contrast agents has been shown to be superior to unenhanced imaging and helical CT for detecting metastatic disease [12,32,33]. Conventional 2D sequences have been widely used for DGEI but they are handicapped by relatively thick sections and inter-section gaps, which limits the diagnosis of sub-cm lesions. The recent introduction of fast 3D T1w GRE sequences has overcome many of these problems [34]. Current 3D sequences result in a higher SNR and thinner effective slice thickness than 2D methods without inter-slice gap or cross-talk and comfortably allow thin section coverage of the whole liver in a single breathhold (Fig. 2). Such sequences are now available from most manufacturers (Siemens VIBE, Philips WAVE, GE FAME). Use of a short repetition time (≈4 ms), and echo time (≈1.6 ms) combined with interpolation algorithms, allows higher resolution matrices and a thinner effective slice thickness with minimal time penalties. The intermittent application of a chemically selective fat saturation (FS) pulse before each partition loop achieves homogeneous fat suppression. This is particularly important for DGEI because effective FS increases the dynamic range within the image and accentuates gadolinium enhancement. A flip angle (FA) of approximately 15° is chosen to minimise the saturation of stationary tissues for the simultaneous display of liver parenchyma and hepatic vessels [35]. Flexible parameters allow scan times to be adjusted to accommodate the breathhold capacity of individual patients, and can also be manipulated to produce isotropic voxels for optimum 3D reconstruction. Isotropic voxels are achieved at the expense of anatomic coverage but this is largely overcome by parallel imaging techniques. In most cases a parallel imaging factor of two enables isotropic imaging of the whole liver in approximately 20 s.

Imaging with Gd should include baseline pre-contrast images and sequential acquisitions at arterial, portal and equilibrium phases. The arterial phase is the most crucial acquisition and the timing should be optimised by test bolusing wherever possible [36]. Best results are obtained when the contrast is administered by a power injector at a rate of 2–4 ml per second followed by a saline flush.

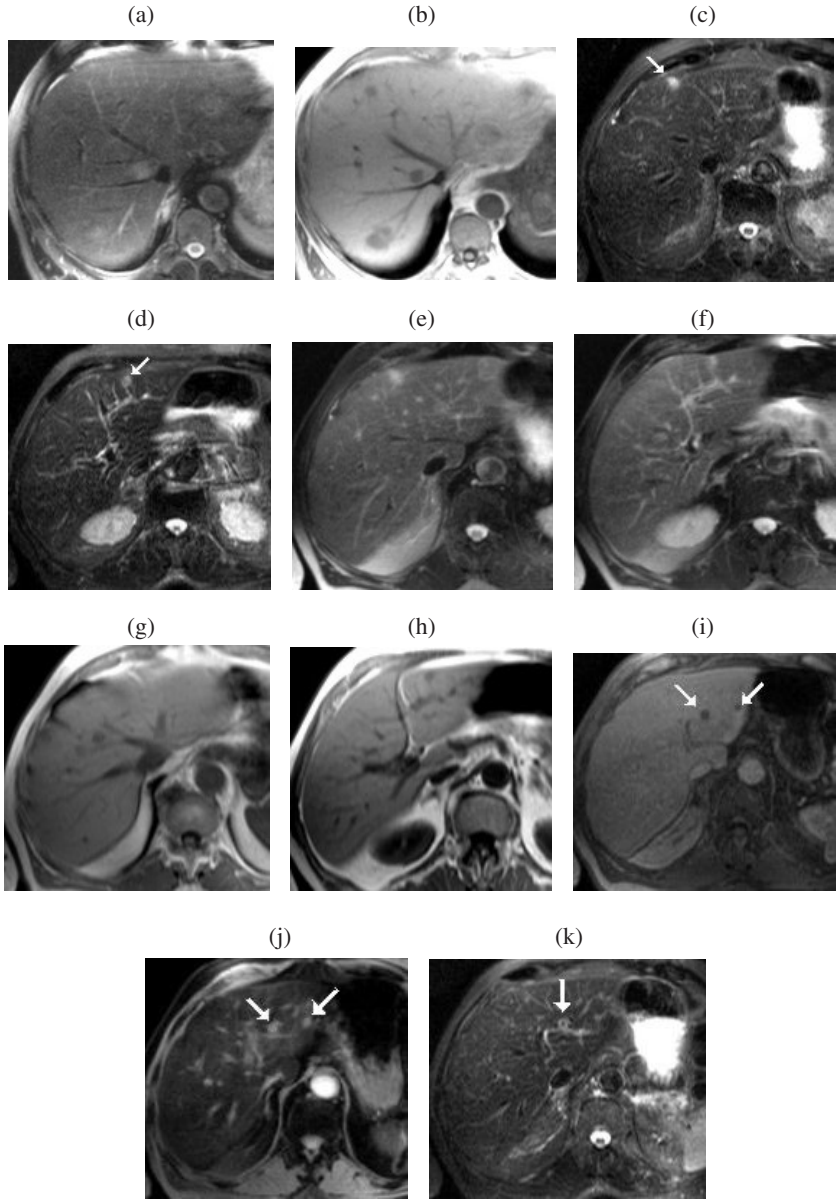

Figure 1 **Relative liver-to-lesion contrast on unenhanced breathhold (BH) imaging. BH T2w FSE (a) illustrating poor visibility of multiple metastases. The lesions are more conspicuous on the corresponding IPT1w images. (b) In a second patient also with multiple small metastases, two left lobe lesions (arrows) are highly conspicuous on BH STIR ((c) and (d)). Both lesions are visible on BH FSE ((e) and (f)) and IPT1w ((g) and (h)) but with reduced liver-to-lesion contrast compared with STIR. Two additional sub-cm lesions (arrows) are well seen on SPIO-enhanced 3D FS T1w (i) and T2w GRE images (j) but only one is seen on the corresponding STIR image (k).**

Hypervascular metastases are most conspicuous at the arterial phase when there is only minimal enhancement of background liver and many are only visible at this time. Most hypovascular lesions are best demonstrated at the portal phase when liver enhancement is maximum but these lesions usually exhibit a transient rim of enhancement which is highly specific for metastases and often only visible at the earlier arterial phase (Fig. 3). An optimised arterial phase is also important for identifying sub-cm metastases and distinguishing them from benign lesions. Compared with simple cysts which exhibit non-progressive enhancement and haemangiomas which show discontinuous and persistent enhancement, metastases have a progressive enhancement pattern and become either less conspicuous over time or more conspicuous as a result of delayed central enhancement due to non-specific accumulation of contrast within the lesion's extra-cellular space. Most small metastases become less distinct and apparently smaller on subsequent acquisitions. By the equilibrium phase contrast between

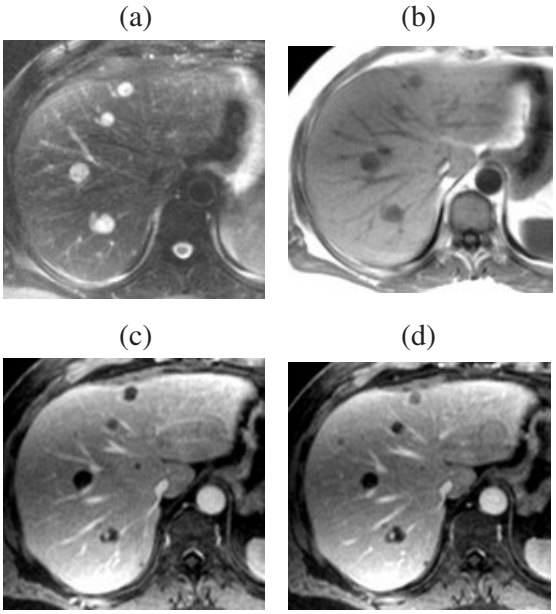

Figure 2 **Dynamic Gd-enhanced MR versus unenhanced MR for lesion detection—role of 3D FS T1w GRE imaging. In a patient with pancreatic cancer several metastases larger than 1 cm are well seen on BH T2 FSE (a) and IPT1w (b) images. Adjacent thin-slice (2.5 mm) portal phase post-Gd 3D FS T1w GRE images ((c) and (d)) obtained at the same level as ((a) and (b)) clearly show several additional previously undetected sub-cm metastases.**

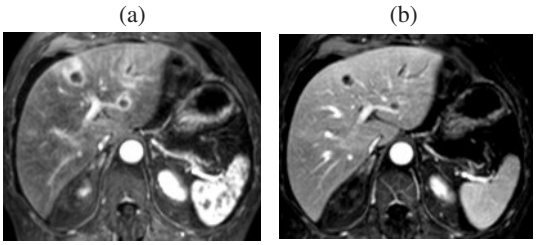

Figure 3 **Value of arterial phase for characterising and delineating hypovascular metastases. Characteristic continuous rim enhancement is clearly seen on arterial phase post-Gd 3D FS T1w GRE images (a). The lesions are still conspicuous by the portal phase (b) but the enhancing rim is less apparent and the lesions appear smaller.**

normal and abnormal tissue is generally poor and many lesions are no longer visible.

Delayed Gd-enhanced imaging with FS is the technique of choice for demonstrating small metastases on the liver surface. Fat suppression not only accentuates gadolinium enhancement but also suppresses the competing high signal of intra-abdominal fat adjacent to the liver surface. Surface deposits are usually best seen on delayed images acquired 5–10 min after injection when they become hyperintense due to slow accumulation of contrast within the tumour[37] (Fig. 4).

In patients with metastatic disease, however, the main role of DGEI is probably to differentiate benign and malignant lesions. DGEI is the most reliable method for characterising lesions and is recommended in all surgical candidates with equivocal lesions in a location which is likely to influence the surgical approach. The perfusion and extraction characteristics of tissues at the different phases of enhancement allow the differentiation of cysts, haemangiomas, FNH and metastases and a specific diagnosis is possible in most patients[38,39].

Tissue-specific contrast agents

Liver-specific contrast agents were developed to increase and prolong lesion-liver contrast beyond that of the ECS agents. A minority of lesions have perfusion characteristics similar to normal liver and are occult on DGEI. Also many small lesions are no longer visible by the equilibrium phase when contrast is evenly distributed between intravascular and extra-cellular spaces. All liver-specific agents produce high tissue contrast and have been shown significantly to improve the detection of metastases compared with unenhanced MR, with enhanced MR using ECS agents with 2D GRE sequences and with contrast-enhanced CT[13–25,40–44]. Agents which target the hepatocytes and produce positive enhancement on T1w images (gadobenate, gadoxetic acid, mangafodipir) and superparamagnetic iron oxide (SPIO) agents (ferumoxides, ferucarbotran), which target the Kupffer cells and cause a marked signal loss on T2w GRE images, are currently available. In terms of lesion detection, metastases are more conspicuous after contrast enhancement because malignant lesions lack functioning hepatocytes or Kupffer cells; whilst lesion signal intensity is unchanged the surrounding liver becomes either hyperintense (T1 agents) or hypointense (SPIO). Gadobenate (Gd-BOPTA, Multihance, Bracco) and gadoxetic acid (Gd-EOB-DPTA, Primovist, Schering) have a biphasic enhancement profile. Both behave like ECS Gd in the first few minutes after injection and exhibit hepatocyte selectivity on delayed phase images[45]. Both phases are recommended to maximise sensitivity but the detection of small metastases is better on delayed images than on the early vascular phases[46] (Fig. 5). Maximum contrast between normal and abnormal tissue occurs 40–120 min and 10–40 min after injection of gadobenate and gadoxetic acid respectively. Compared with unenhanced images mangafodipir trisodium (Mn-DPDP, Teslascan, Nycomed Amersham) also improves lesion detection[40]. Lesion-to-tumour contrast is maximal between 15 min and 2 h after injection but some metastases may be most conspicuous on 24 h images due to delayed washout around their periphery (Fig. 6). T1w GRE imaging is recommended for all three hepatocyte agents. At the time of writing no comparative studies have evaluated the accuracy of these agents using high-resolution 3D T1w GRE imaging but it is likely that the better spatial

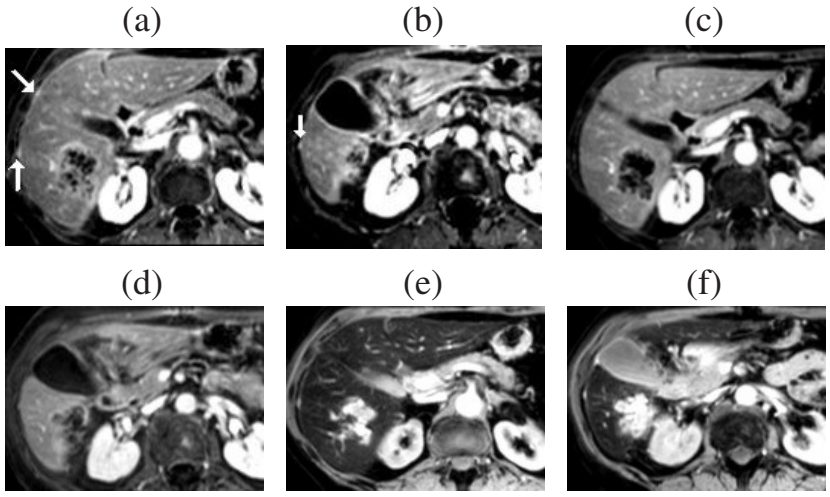

Figure 4 **Role of Gd-enhanced delayed imaging with fat suppression for detecting small metastases on the liver surface. In a patient with colorectal cancer small surface deposits (arrows) are well seen on 3D FS T1w GRE images obtained approximately 10 min after Gd ((a) and (b)). The lesions are not visible on the earlier portal phase images ((c) and (d)). Surface lesions are also highly conspicuous on FS T2w GRE images following SPIO ((e) and (f)).**

resolution provided by this sequence will improve the detection of sub-cm lesions compared with 2D sequences.

MRI enhanced with SPIO is probably the most sensitive method for detecting hepatic metastases[13–26,35]. In the few studies which have compared the different liver specific agents against each other, SPIO-enhanced MRI has demonstrated varying degrees of superiority, particularly for small lesions[25,47]. Two SPIO agents are available for liver MR, ferumoxides (AMI-25, Endorem, Guerbet) and ferucarbotran (SHU 555A, Resovist, Schering). Both agents have a particle size of 30–200 nm which results in approximately 80% of the injected dose being taken up by the normal liver. When the particles are clustered within the Kupffer cells they induce local field inhomogeneities which lead to rapid spin dephasing and a reduction in signal on both T1w and T2w images although the effect is most pronounced on T2w due to a high R2/R1 ratio. While metastases retain their high SI on T2w images the signal of the background liver is dramatically reduced, so tumour-to-liver contrast is markedly increased. Signal loss after SPIO increases with field strength and depends on the type of sequence used. The effect of SPIO is more pronounced on GRE than FSE sequences due to the greater sensitivity of GRE to susceptibility effects. Conversely SPIO enhancement is less with FSE sequences because multiple closely spaced refocusing pulses diminish the local field inhomogeneities induced by the SPIO particles. MT effects which reduce the SI of solid lesions are also a feature of FSE but not GRE sequences. Although the effect of SPIO is maximised with GRE imaging, best results are obtained when parameters are optimised to minimise noise and maximise the signal from solid lesions. In a recent multi-observer study optimised T2w breathhold SPIO-enhanced FSE and GRE sequences were compared with unenhanced images, for the detection of surgically confirmed metastases[27]. Whilst the best GRE sequence achieved accuracies of 93% for all lesions and 82% for sub-cm lesions, enhanced FSE was no better than unenhanced images and achieved accuracies of 82% and 64% for all lesions and sub-cm lesions respectively. On the basis of these results the authors now use only this optimised GRE sequence with SPIO. However, in an attempt to improve the detection of sub-cm and surface lesions the sequence has been further refined by reducing the slice thickness from 10 to 6 mm and applying fat suppression (Fig. 7). The details of this sequence are as follows: TR 148 ms, TE14 ms, FA 30°, BW 65–80 Hz/pixel, 65% phase resolution combined with a 68%–75% rectangular 280–400 mm field of view to achieve a 132 × 256 matrix and flow compensation. The low bandwidth is used to minimise noise and increase SNR whilst flow compensation gradients minimise flow artifact. The flip angle is based on the Ernst angle (the FA at which maximum signal for any tissue occurs) for hepatic metastases at 1.5 T and a T1 of 1000 ms. More recently, this SPIO-enhanced sequence was compared with high-resolution 3D FS T1w DGEI and thin-slice contrast-enhanced helical CT for detecting hepatic metastases using histopathology and surgery with IOUS as the reference standard[35]. Overall the two MR techniques showed similar accuracies and both were significantly more accurate than CT, but the detection of lesions 1 cm or smaller was substantially improved with SPIO.

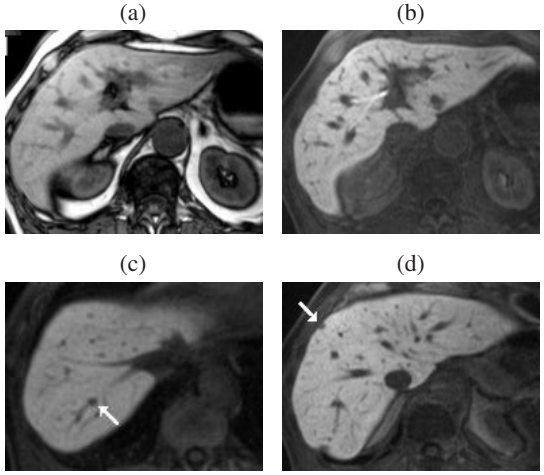

Figure 5 **Multiple metastases—improved detection with Gd-EOB-DTPA at the hepatocyte phase of enhancement. Compared with non-contrast T1w images (a) liver-to-lesion contrast is improved on 20 min post-contrast T1w images (b). Additional surgically confirmed sub-cm lesions (arrows) were only visible on hepatocyte phase images ((c) and (d)). Adapted with permission from Robinson PJA, Ward J (2006) MRI of the Liver: A Practical Guide. Informa Healthcare, New York.**

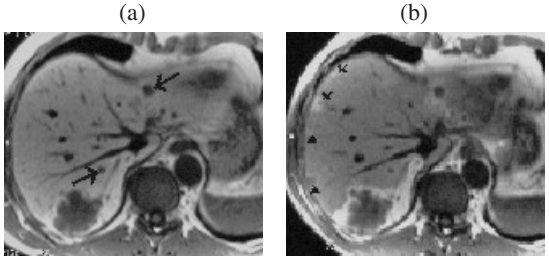

Figure 6 **Improved detection of metastases with 24 h mangafodipir-enhanced imaging. Multiple metastases (arrows) are seen with high lesion-to-liver contrast on 20 min post-mangafodipir T1w 2D GRE images (a). However several additional lesions are only visible on the corresponding images obtained 24 h after contrast (b) when the background liver signal has returned to normal, due to retained contrast in the compressed liver tissue at the periphery of the lesions. (Images courtesy of Dr J. Healy.)**

The choice of SPIO agent is also important. Ferucarbotran is given by bolus injection and provides the opportunity to obtain dynamic T1w images in the first few minutes after injection[48]. At this time, because the iron oxide particles are distributed within the intravascular space and less concentrated they produce T1w enhancement on T1w images. Liver-to-lesion contrast is maximum on delayed T2w images when the particles are clustered within the RE cells and more concentrated, but we have found this early T1 enhancement on 3D FS T1w GRE images to be particularly valuable for depicting small tumours. The T1 effect is usually considerably less than occurs with ECF Gd agents but this is often beneficial in the context of metastatic disease. Liver and vessels often have a similar SI which produces a virtual 'blank canvas' against which small metastases are extremely conspicuous and reliably distinguished from vessels (Fig. 8). In the author's experience the combination of thin-slice 3D T1w and T2w imaging after SPIO increases diagnostic confidence and is more accurate for small lesion detection than delayed T2w imaging alone, although there are currently no published data to support this view. We have also found that optimised FS T2w GRE imaging after SPIO is of value in depicting extra-hepatic and peritoneal tumour deposits which are well seen against the suppressed signal of fat and the reduced liver signal after SPIO (Fig. 4).

The most efficient method of FS involves the selective excitation of water protons using a binomial pulse sequence. Compared with the standard frequency selective method of FS this approach is less sensitive to magnetic field inhomogeneities and allows more slices to be obtained for a given acquisition time[49]. We have found that, regardless of the position of the imaging slab, manual shimming close to the isocentre achieves homogeneous FS even at more peripheral levels where the main magnetic field is less homogeneous.

The true accuracy of imaging and future developments

All liver metastases start out as microscopic seedlings which eventually grow to a size where they become visible on imaging. According to surveillance studies the mean age of synchronous metastases at the time of surgery for the primary tumour is approximately 2–3 years. Most lesions larger than a centimetre are depicted on all imaging techniques but the detection of sub-cm metastases is still disappointing. Using optimum technique, high contrast lesions of 2–3 mm can be detected but metastases (which have low contrast) in this size range are rarely visualised. Although there is no expectation that current imaging techniques will depict metastases of millimetre size, detection rates of 85%–90% are consistently reported for CT and MR. The literature on liver imaging is generally limited by inadequate methods for verifying findings and in most studies false negative lesions are not assessed. This inevitably means that reported sensitivities are overestimated and that the true incidence of disease is underestimated. Moreover, in more recent studies investigators have attempted to judge their results against more rigorous reference standards so there has been little if any improvement in apparent sensitivities despite continuing improvements in imaging techniques. It is also likely that these results continue to underestimate the problem of metastases in the millimetre size range and

reported sensitivities remain falsely elevated. Even when histological examination of the resected liver is used as the 'gold standard' the verification of very small lesions is questionable since most specimens are sectioned at 1 cm intervals. Furthermore, recent follow-up studies have confirmed that a proportion of small metastases are undetected by preoperative imaging and surgery with IOUS. In two studies referred to previously[27,35] approximately 15% of patients were found to have 'new' tumours on follow-up CT performed 4–6 months after hepatic resection. It is likely that these metastases were present at the time of surgery but missed by preoperative imaging and by surgical inspection with IOUS. A meticulous correlation with surgery and histology of the resected specimen sectioned at 3 mm intervals showed that 24%[35] and 18%[27] of lesions 1 cm or smaller were not detected by any imaging technique. Moreover for the detection of small lesions, the results of both studies compared favourably with those of earlier studies in which a specific analysis of sub-cm lesions was performed[7,10,13,20,24].

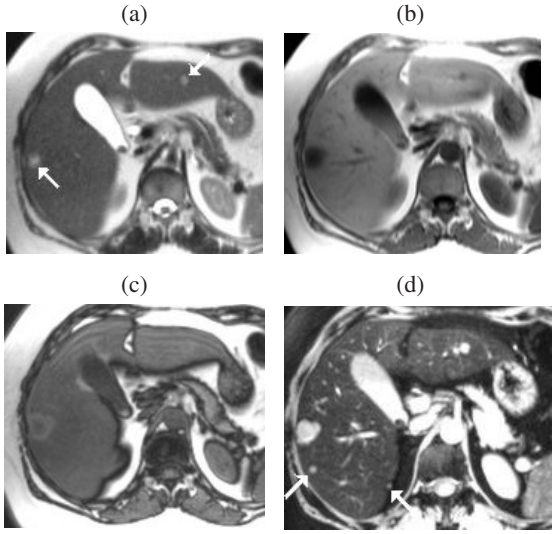

Figure 7 **Improved detection of small metastases with optimised SPIO-enhanced T2w GRE imaging. In a patient with colorectal metastases and a fatty liver, right and left lobe lesions (arrows) are well seen on HASTE (a) and IPT1w (b) images. The lesions are isointense against the reduced signal of the adjacent fatty liver on OPT1w (c). Additional small metastases (arrows) not seen on (a–c) are clearly seen on SPIO-enhanced T2w GRE images (d) acquired with a 6 mm slice thickness and fat suppression.**

On 'state-of-the-art' systems 3D sequences can achieve full liver coverage with isotropic voxels of 1 mm in a breathhold. However, SNR decreases with decreasing voxel size so lesion contrast is degraded by noise. The higher SNR provided by 3.0 T technology (SNR at 3.0 T is twice that at 1.5 T) has the potential to improve contrast resolution but increased power deposition, decreased RF field uniformity and distortion artifacts due to increased susceptibility are problematic. Hepatocyte-specific agents used with 3D T1w sequences combine high tissue contrast with improved spatial resolution and may rival SPIO-enhanced T2w imaging for the detection of small metastases but they are unlikely to outperform SPIO when high-resolution T1w and T2w images are combined.

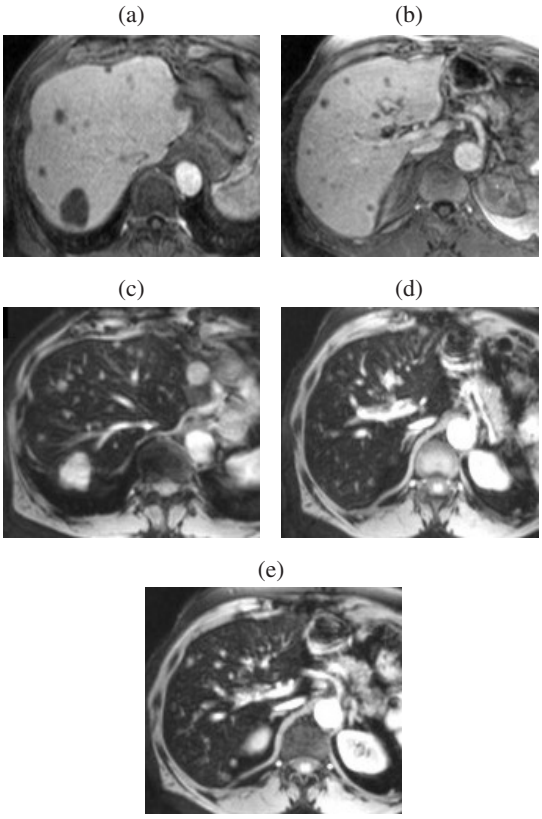

Figure 8 **Value of dynamic high-resolution T1w imaging with ferucarbotran for depicting small metastases. Multiple small metastases (many not visible on unenhanced images) are highly conspicuous on 3D FS T1w GRE imaging (effective slice thickness 2.5 mm) obtained 45 s after bolus injection of ferucarbotran ((a) and (b)). Note the relatively weak T1 effect resulting in isointensity of the background liver and vessels. The lesions are also well seen on corresponding T2w GRE images (c–e) obtained 10 minutes after (a) and (b).**

Data on the use of diffusion weighted imaging (DWI) for liver lesion detection are limited. Variable image quality caused by motion artifacts and reduced SNR have largely restricted applications to differentiating benign and malignant lesions (benign lesions have higher apparent diffusion coefficients than malignant lesions). Also, most diffusion weighted sequences are acquired with a slice thickness of 7–8 mm so the detection of small metastases is limited. However, recent work suggests that DWI using small b-values to produce black blood images improves the differentiation of small metastases

and vessels on T2w images and is more sensitive than T2w FSE sequences for lesion detection[50].

Clearly, continuing improvements in imaging are allowing metastases to be identified at an earlier stage but a different approach is needed to improve the detection of metastases smaller than 2 mm. Hepatic perfusion indexing (HPI) using nuclear medicine and ultrasound techniques[51,52] has had success in identifying metastases before they become evident on conventional imaging. Patients with liver metastases have increased arterial blood flow and a higher arterial/portal ratio (the HPI) than those with a normal liver. Several animal studies indicate that the increase in hepatic arterial fraction occurs shortly after metastatic seeding and reliably predicts the development of overt metastases[53,54]. Early results in patients were promising but subsequent studies produced varied findings and showed substantial intra-observer variability so neither technique has found acceptance in routine practice. More recently MR has been used to measure HPI[55,56] but the technique remains developmental and the best measurement method is still to be determined. Once the methodology is established rigorous multi-observer studies will be required to validate the technique and determine its impact on patient management.

Recommendations

The author's experience has evolved in a centre which provides a supra-regional service for liver surgery. In patients who are candidates for hepatic resection our current practice is to perform unenhanced IP and OPT1w GRE and HASTE sequences followed by dynamic SPIO-enhanced 3D FS T1w GRE imaging and delayed T2w GRE sequences. If a lesion has benign characteristics on HASTE and a location which may influence the surgical approach we perform DGEI immediately after SPIO-enhanced imaging for more reliable characterisation. In non-surgical patients or patients with rising tumour markers unenhanced imaging followed by high-resolution DGEI is preferred.

Acknowledgements

The author thanks Professor P. J. Robinson for his review of the manuscript and helpful comments and Mrs S Boyes for her help in preparing the manuscript.

References

[1] Malafosse R, Penna C, Sa Cunha A, Nordlinger B. Surgical management of hepatic metastases from colorectal malignancies. Ann Oncol 2001; 12: 887–94.

[2] Miyazaki M, Ito H, Nakagawa K, Ambiru S, Shimizu H, Okuno A *et al*. Aggressive surgical resection for hepatic metastases involving the inferior vena cava. Am J Surg 1999; 177: 294–8.

[3] Lodge JP, Ammori BJ, Prasad KR, Bellamy MC. Ex vivo and in situ resection of inferior vena cava with hepatectomy for colorectal metastases. Ann Surg 2000; 231: 471–9.

[4] Jaeck D, Bachellier P, Guiguet M, Boudjema K, Vaillant JC, Balladur P *et al*. Long-term survival following resection of colorectal hepatic metastases. Br J Surg 1997; 84: 977–80.

[5] Harrison LE, Brennan MF, Newman E, Fortner JG, Picardo A, Blumgart LH *et al*. Hepatic resection for noncolorectal, nonneuroendocrine metastases: a fifteen-year experience with ninety-six patients. Surgery 1997; 121: 625–32.

[6] Miyazaki M, Itoh H, Nakagawa K, Ambiru S, Shimizu H, Togawa A *et al*. Hepatic resection of liver metastases from gastric carcinoma. Am J Gastroenterol 1997; 92: 490–3.

[7] Kuszyk BS, Bluemke DA, Urban BA, Choti MA, Hruban RH, Sitzmann JV *et al*. Portal-phase contrast-enhanced helical CT for the detection of malignant hepatic tumors: sensitivity based on comparison with intra-operative and pathologic findings. AJR Am J Roentgenol 1996; 166: 91–5.

[8] Valls C, Lopez E, Guma A, Gil M, Sanchez A, Andia E *et al*. Helical CT versus CT arterial portography in the detection of hepatic metastasis of colorectal carcinoma. AJR Am J Roentgenol 1998; 170: 1341–7.

[9] Ward J, Naik KS, Guthrie JA, Wilson D, Robinson PJ. Hepatic lesion detection: comparison of MR imaging after the administration of superparamagnetic iron oxide with dual-phase CT by using alternative-free response receiver operating characteristic analysis. Radiology 1999; 210: 459–66.

[10] Valls C, Andia E, Sanchez A, Guma A, Figueras J, Torras J *et al*. Hepatic metastases from colorectal cancer: preoperative detection and assessment of resectability with helical CT. Radiology 2001; 218: 55–60.

[11] Furuhata T, Okita K, Tsuruma T, Hata F, Kimura Y, Katsuramaki T *et al*. Efficacy of SPIO-MR imaging in the diagnosis of liver metastases from colorectal carcinomas. Dig Surg 2003; 20: 321–5.

[12] Semelka RC, Cance WG, Marcos HB, Mauro MA. Liver metastases: comparison of current MR techniques and spiral CT during arterial portography for detection in 20 surgically staged cases. Radiology 1999; 213: 86–91.

[13] Hagspiel KD, Neidl KF, Eichenberger AC, Weder W, Marincek B. Detection of liver metastases: comparison of superparamagnetic iron oxide-enhanced and unenhanced MR imaging at 1.5 T with dynamic CT, intraoperative US, and percutaneous US. Radiology 1995; 196: 471–8.

[14] Seneterre E, Taourel P, Bouvier Y, Pradel J, Van Beers B, Daures JP *et al*. Detection of hepatic metastases: ferumoxides-enhanced MR imaging versus unenhanced MR imaging and CT during arterial portography. Radiology 1996; 200: 785–92.

[15] Muller RD, Vogel K, Neumann K, Hirche H, Barkhausen J, Stoblen F *et al*. SPIO-MR imaging versus double-phase spiral CT in detecting malignant lesions of the liver. Acta Radiol 1999; 40: 628–35.

[16] Lencioni R, Della Pina C, Bruix J, Majno P, Grazioli L, Morana G *et al*. Clinical management of hepatic malignancies: ferucarbotran-enhanced magnetic resonance imaging versus contrast-enhanced spiral computed tomography. Dig Dis Sci 2005; 50: 533–7.

[17] Poeckler-Schoeniger C, Koepke J, Gueckel F, Sturm J, Georgi M. MRI with superparamagnetic iron oxide: efficacy in the detection and characterization of focal hepatic lesions. Magn Reson Imaging 1999; 17: 383–92.

[18] Ba-Ssalamah A, Heinz-Peer G, Schima W, Schibany N, Schick S, Prokesch RW *et al*. Detection of focal hepatic lesions: comparison of unenhanced and SHU 555 A-enhanced MR imaging versus biphasic helical CTAP. J Magn Reson Imaging 2000; 11: 665–72.

[19] Reimer P, Jahnke N, Fiebich M, Schima W, Deckers F, Marx C *et al*. Hepatic lesion detection and characterization: value of nonenhanced MR imaging, superparamagnetic iron oxide-enhanced MR imaging and spiral CT-ROC analysis. Radiology 2000; 217: 152–8.

[20] Ward J, Chen F, Guthrie JA, Wilson D, Lodge JP, Wyatt JI *et al*. Hepatic lesion detection after superparamagnetic iron oxide enhancement: comparison of five T2-weighted sequences at 1.0 T by using alternative-free response receiver operating characteristic analysis. Radiology 2000; 214: 159–66.

[21] van Etten B, van der Sijp J, Kruyt R, Oudkerk M, van der Holt B, Wiggers T. Ferumoxide-enhanced magnetic resonance imaging techniques in pre-operative assessment for colorectal liver metastases. Eur J Surg Oncol 2002; 28: 645–51.

[22] Kim MJ, Kim JH, Chung JJ, Park MS, Lim JS, Oh YT. Focal hepatic lesions: detection and characterization with combination gadolinium and superparamagnetic iron oxide-enhanced MR imaging. Radiology 2003; 228: 719–26.

[23] Takahama K, Amano Y, Hayashi H, Ishihara M, Kumazaki T. Detection and characterization of focal liver lesions using superparamagnetic iron oxide-enhanced magnetic resonance imaging: comparison between ferumoxides-enhanced T1-weighted imaging and delayed-phase gadolinium-enhanced T1-weighted imaging. Abdom Imaging 2003; 28: 525–30.

[24] Vogl TJ, Schwarz W, Blume S, Pietsch M, Shamsi K, Franz M *et al*. Preoperative evaluation of malignant liver tumors: comparison of unenhanced and SPIO (Resovist)-enhanced MR imaging with biphasic CTAP and intraoperative US. Eur Radiol 2003; 13: 262–72.

[25] Kim YK, Lee JM, Kim CS, Chung GH, Kim CY, Kim IH. Detection of liver metastases: gadobenate dimeglumine-enhanced three-dimensional dynamic phases and one-hour delayed phase MR imaging versus superparamagnetic iron oxide-enhanced MR imaging. Eur Radiol 2005; 15: 220–8.

[26] Limanond P, Raman SS, Sayre J, Lu DSK. Comparison of dynamic gadolinium-enhanced and ferumoxides-enhanced MRI of the liver on high- and low-field scanners. J Magn Res Imaging 2004; 20: 640–7.

[27] Ward J, Guthrie JA, Wilson D, Arnold P, Lodge JP, Toogood GJ *et al*. Colorectal hepatic metastases: detection with SPIO-enhanced breath-hold MR imaging comparison of optimized sequences. Radiology 2003; 228: 709–18.

[28] Gaa J, Hatabu H, Jenkins RL, Finn JP, Edelman RR. Liver masses: replacement of conventional T2-weighted spin-echo MR imaging with breath-hold MR imaging. Radiology 1996; 200: 459–64.

[29] Huang J, Raman SS, Vuong N, Sayre JW, Lu DS. Utility of breath-hold fast-recovery fast spin-echo T2 versus respiratory-triggered fast spin-echo T2 in clinical hepatic imaging. AJR Am J Roentgenol 2005; 184: 842–6.

[30] Mitchell DG. Focal manifestations of diffuse liver disease at MR imaging. Radiology 1992; 185: 1–11.

[31] Earls JP, Rofsky NM, DeCorato DR, Krinsky GA, Weinreb JC. Echo-train STIR MRI of the liver: comparison of breath-hold and non-breath-hold imaging strategies. J Magn Reson Imaging 1999; 9: 87–92.

[32] Oi H, Murakami T, Kim T, Matsushita M, Kishimoto H, Nakamura H. Dynamic MR imaging and early-phase helical CT for detecting small intrahepatic metastases of hepatocellular carcinoma. AJR Am J Roentgenol 1996; 166: 369–74.

[33] Blakeborough A, Ward J, Wilson D, Griffiths M, Kajiya Y, Guthrie JA *et al*. Hepatic lesion detection at MR imaging: a comparative study with four sequences. Radiology 1997; 203: 759–65.

[34] Lee VS, Lavelle MT, Rofsky NM, Laub G, Thomasson DM, Krinsky GA *et al*. Hepatic MR imaging with a dynamic contrast-enhanced isotropic volumetric interpolated breath-hold examination: feasibility, reproducibility, and technical quality. Radiology 2000; 215: 365–72.

[35] Ward J, Robinson PJ, Guthrie JA, Downing S, Wilson D, Lodge JP *et al*. Detection of liver metastases in candidates for hepatic resection: comparison of thin-slice helical CT, high-resolution 3D dynamic gadolinium-enhanced MR and SPIO-enhanced T2W gradient echo imaging. Radiology 2005; 237: 170–80.

[36] Earls JP, Rofsky NM, DeCorato DR, Krinsky GA, Weinreb JC. Hepatic arterial-phase dynamic gadolinium-enhanced MR imaging: optimization with a test examination and a power injector. Radiology 1997; 202: 268–73.

[37] Low RN, Barone RM, Lacey C, Sigeti JS, Alzate GD, Sebrechts CP. Peritoneal tumour: MR imaging with dilute oral barium and intravenous gadolinium-containing contrast agents compared with unenhanced MR imaging and CT. Radiology 1997; 204: 513–20.

[38] Hawighorst H, Schoenberg SO, Knopp MV, Essig M, Miltner P, van Kaick G. Hepatic lesions: morphologic and functional characterization with multiphase breath-hold 3D gadolinium-enhanced MR angiography—initial results. Radiology 1999; 210: 89–96.

[39] Low RN. MR imaging of the liver using gadolinium chelates. In: MR Imaging of the Liver 1: Techniques and Contrast Agents. Magn Reson Imaging Clinics N Am 2001; 717–43.

[40] Bartolozzi C, Donati F, Cioni D, Procacci C, Morana G, Chiesa A *et al*. Detection of colorectal liver metastases: a prospective multicenter trial comparing unenhanced MRI, MnDPDP-enhanced MRI and spiral CT. Eur Radiol 2004; 14: 14–20.

[41] Huppertz A, Balzer T, Blakeborough A, Breuer J, Giovagnoni A, Heinz-Peer G *et al*. European EOB Study Group. Improved detection of focal liver lesions at MR imaging: multicenter comparison of gadoxetic acid-enhanced MR images with intraoperative findings. Radiology 2004; 230: 266–75.

[42] Braga HJ, Choti MA, Lee VS, Paulson EK, Siegelman ES, Bluemke DA. Liver lesions: manganese-enhanced MR and dual-phase helical CT for preoperative detection and characterization comparison with receiver operating characteristic analysis. Radiology 2002; 223: 525–31.

[43] Kuwatsuru R, Kadoya M, Ohtomo K, Tanimoto A, Hirohashi S, Murakami T *et al*. Comparison of gadobenate dimeglumine with gadopentetate dimeglumine for magnetic resonance imaging of liver tumors. Invest Radiol 2001; 36: 632–41.

[44] Petersein J, Spinazzi A, Giovagnoni A, Soyer P, Terrier F, Lencioni R *et al*. Focal liver lesions: evaluation of the efficacy of gadobenate dimeglumine in MR imaging—a multicenter phase III clinical study. Radiology 2000; 215: 727–36.

[45] Reimer P, Schneider G, Schima W. Hepatobiliary contrast agents for contrast-enhanced MRI of the liver: properties, clinical development and applications. Eur Radiol 2004; 14: 559–78.

[46] Kim YK, Lee JM, Kim CS. Gadobenate dimeglumine-enhanced liver MR imaging: value of dynamic and delayed imaging for the characterization of focal liver lesions. Eur Radiol 2004; 14: 5–13.

[47] Kim MJ, Kim JH, Lim JS, Oh YT, Chung JJ, Choi JS *et al*. Detection and characterization of focal hepatic lesions: mangafodipir vs. superparamagnetic iron oxide-enhanced magnetic resonance imaging. J Magn Reson Imaging 2004; 20: 612–21.

[48] Reimer P, Balzer T. Ferucarbrotran (Resovist): a new clinically approved RES-specific contrast agent for contrast-enhanced MRI of the liver: properties, clinical development and applications. Eur Radiol 2003; 13: 1266–76.

[49] Sala E, Graves MJ, Jardine VL, Loubert I, Lomas DJ. Abdominal MRI: evaluation of binomial water excitation for fat suppression. Proc Intl Soc Mag Reson Med 2003; 1130.

[50] Hussain SM, De Becker J, Hop WC, Dwarkasing S, Wielopolski PA. Can a single-shot black-blood T2-weighted spin-echo echo-planar imaging sequence with sensitivity encoding replace the respiratory-triggered turbo spin-echo sequence for the liver? An optimization and feasibility study. J Magn Reson Imaging 2005; 21: 219–29.

[51] Parkin A, Robinson PJ, Baxter P, Leveson SH, Wiggins PA, Giles GR. Liver perfusion scintigraphy-method, normal range, and laparotomy correlation in 100 patients. Nucl Med Commun 1983; 72: 128–30.

[52] Leen E, Angerson WJ, Wotherspoon H, Moule B, Cook TG, McArdle CS. Detection of colorectal liver metastases: comparison of laparotomy, CT, US and Doppler perfusion index and evaluation of postoperative follow-up results. Radiology 1995; 195: 113–6.

[53] Cuenod C, Leconte I, Siauve N, Resten A, Dromain C, Poulet B *et al*. Early changes in liver perfusion caused by occult metastases in rats: detection with quantitative CT. Radiology 2001; 218: 556–61.

[54] Hemingway DM, Cooke TG, Grime SJ, Nott DM, Jenkins SA. Changes in hepatic haemodynamics and hepatic perfusion index during the growth and development of hypovascular HSN sarcoma in rats. Br J Surg 1991; 78: 326–30.

[55] Materne R, Smith AM, Peeters F, Dehoux JP, Keyeux A, Horsmans Y *et al*. Assessment of hepatic perfusion parameters with dynamic MRI. Magn Reson Med 2002; 47: 135–42.

[56] Totman JJ, O'gorman RL, Kane PA, Karani JB. Comparison of the hepatic perfusion index measured with gadolinium-enhanced volumetric MRI in controls and in patients with colorectal cancer. Br J Radiol 2005; 78: 105–9.